

ORIGINAL RESEARCH PAPER

# An Analytical Approach for Modeling Fluid-structure Interaction Problems in Axisymmetric Domains

H. Afrasiab\*

Mechanical Engineering Department, Babol Noshirvani University of Technology, Babol, Iran.

## Article info

### Article history:

Received 10 January 2022

Received in revised form

25 February 2022

Accepted 09 March 2022

### Keywords:

Fluid-structure interaction

Analytical solution

Axisymmetric domain

Stress variation

## Abstract

Few analytical approaches have been proposed so far for solving Fluid-Structure Interaction (FSI) problems in the literature. In fact, FSI is generally so complicated that its analytical solution remains almost unavailable. Inspired by this fact, here an analytical methodology is presented for modeling steady-state fluid-structure interaction problems in axisymmetric domains. For this purpose, the Navier-Stokes equations for the flow of the incompressible viscous fluid, and the linear elasticity equations for the deformation of the solid structure are expressed in axisymmetric coordinates. Appropriate boundary conditions are also employed that are capable of coupling the fluid and solid domains by imposing kinematic and dynamic constraints on the fluid-structure interaction interface. The set of fluid and structure equations are solved by MATLAB symbolic toolbox. The accuracy of the presented analytical approach is verified in two different ways. First, by specializing the results for the simple case of a thick cylindrical pressure vessel, second, by comparing the analytical results for flow through a nozzle with numerical results obtained by ANSYS/CFX simulation. Variation of the stress components is obtained in the nozzle wall. The results of the analytical approach are in good agreement with those of the numerical modeling. The proposed methodology can be used for fast yet efficient solution of fluid-structure interaction problems in axisymmetric configuration.

## Nomenclature

$b$	Volume force per unit mass, N/kg	$E$	Modulus of elasticity, N/m <sup>2</sup>
$I$	Unit tensor	$p$	Fluid pressure, N/m <sup>2</sup>
$r$	Radial coordinate, m	$R$	Radius of fluid domain at FSI interface
$t$	Time, s	$u$	Solid radial displacement, m
$v$	Fluid velocity, m/s	$w$	Solid axial displacement, m
$z$	Axial coordinate, m		
Greek symbols			
$\varepsilon$	Strain tensor	$\mu$	Fluid viscosity, Pa.s
$\nu$	Poissons ratio	$\rho$	Density, kg/m <sup>3</sup>
$\sigma$	Cauchy stress tensor, MPa		

\*Corresponding author: H. Afrasiab (Associate Professor)

E-mail address: afrasiab@nit.ac.ir

<http://dx.doi.org/10.22084/jrstan.2022.26064.1204>

ISSN: 2588-2597

Subscript			
$f$	Fluid	$i$	In
$o$	Out	$r$	Radial
$s$	Solid	$z$	Axial
$\theta$	Angular		

## 1. Introduction

Fluid-Structure Interaction (FSI) which deals with the interaction of some movable or deformable structures with an internal or surrounding fluid flow is encountered in many branches of science and engineering. This phenomenon plays an important role in many engineering problems including the fluttering of aircraft wings [1], deflection of wind-turbine blades [2], inflation of automobile air-bags [3], dynamics of spacecraft parachutes [4], motion of ships [5], performance of pumps and micropumps [6], blood flow and arterial dynamics in healthy and diseased (stenotic or aneurysmal) arteries [7, 8], and lubrication [9] studies.

Fluid-structure interaction has been a hot research topic in recent years. Research on this topic is mainly performed by three types of techniques: experimental, analytical, and numerical. The experimental approach requires the simultaneous measuring of the flow properties and the structural change which is often challenging. Furthermore, experiments are expensive, time consuming, and usually do not allow much flexibility in parameter variation. Consequently, this approach has been mostly used in combination with, or as a verification tool for analytical or numerical approaches, e.g. in [10–12]. On the other hand, with the increasing capacity of numerical computation facilities and the new mathematical algorithms, the numerical approach has received the maximum attention in the related literature, and numerical techniques such as the finite element method [13, 14], the finite volume method [15], the boundary element method [16, 17], the immersed boundary method [18], the extended finite element method [19], the lattice Boltzmann method [20], the smooth particle hydrodynamic method [21] and their combination [22–26] have been used extensively to study different FSI problems.

While numerical simulation is considered to be the most effective approach for solving many practical problems, the most accurate solutions is obtained by using the analytical techniques. Analytical techniques also provide a better understanding of the physical behavior of the system and offer faster computations [27]. Unfortunately, FSI is so complicated that its analytical solution remains almost unavailable. The complexity lies not only in the highly nonlinear response of both the fluid and structure, but also in the behavior of the coupled FSI system [28, 29]. As a consequence, only few analytical solutions are presented in the literature for FSI problems, most of which are limited to

extremely simplified cases.

Xu and Wellens in [30] developed an analytical model to explore the nonlinear fluid-structure interaction between large-scale polymer offshore floating photovoltaics and waves. The floating structure was modeled as a nonlinear Euler Bernoulli-von Kármán beam coupling with water beneath. A multi-time-scale perturbation method was employed leading to hierarchic partial differential equations by introducing the wave steepness squared as the perturbation. The analytical solution of the proposed nonlinear FSI model was obtained up to the second order. Soni et al. in [31] used an analytical approach to study the effect of fluid-structure interaction on vibration and deflection of generally orthotropic submerged micro-plate with crack under thermal environment. The proposed analytical model was based on Kirchhoff's classical thin plate theory and the size effect was introduced using the modified couple stress theory. The fluid forces associated with its inertial effects were added in the governing differential equation to incorporate the fluid-structure interaction effect. Fritsche et al. in [32] proposed an analytical model to investigate the fluid structure interaction of an elastic beam in a water channel. For this purpose, the beam deformation was estimated based on the analytical equations from structural mechanics and an assumed stagnation pressure on the beam surface. Additionally, the drag coefficient from experimental data of the literature was used to estimate the force on and the bending of the beam. Jain et al. in [33] presented an analytical solution for vibration analysis of orthotropic and FGM submerged cylindrical shell containing a surface crack of variable angular orientation with consideration of fluid-structure interaction. The governing equations in terms of transverse deflection of cracked-submerged shell were derived using classical shell theory. The fluid forces associated with its inertial effects were added in the governing differential equation to incorporate the fluid-structure interaction effect. Yu and Whittaker in [34] reviewed the analytical studies on seismic fluid-structure interaction of base-supported cylindrical tanks. They calculated and compared FSI responses for a range of tank dimensions using the analytical solutions from different studies. The responses were normalized to be unitless to be used for tanks with different dimensions and mechanical properties, and subjected to different input motions. Zhang in [35] proposed a simple idea to include fluid-structure interaction (FSI) in classic rectilinear flow problems. Dynamic FSI problems amenable to analytical meth-

ods were obtained by allowing a solid boundary to behave as a rigid body, instead of holding it at constant motions. Four examples including Stokes's first problem, Couette flow, rotating disk, and rotating sphere were analytically solved by Laplace transform.

While several analytical solutions have been presented in the literature to solve the fluid flow and the solid deformation in axisymmetric problems, based on the above literature review and to the best knowledge of the author, such analytical solutions do not exist for the coupled problem of the fluid-structure interaction. Therefore, developing an analytical model that can analytically solve the axisymmetric fluid-structure interaction problems with low computational cost and reasonable accuracy is the main contribution and novelty of the current study. Here, it is aimed to develop a simple yet effective methodology for modeling fluid-structure interaction in axisymmetric domains. The fluid flow in circular pipes, tubes, nozzles, and healthy or diseased arteries are some examples of axisymmetric FSI problems. In this methodology, the steady flow of the incompressible viscous fluid is given by Navier-Stokes equations while the deformation of the solid structure is described by the equations of linear elasticity. The details of the mathematical formulation is described in section 2.

## 2. The Mathematical Formulation

The following assumptions are made for developing the problem formulation in the analytical approach:

- The problem domain is axisymmetric with respect to the  $z$  axis as shown in Fig. 1. The radial and axial components of different variables are specified by  $r$  and  $z$  subscripts, respectively.
- The problem is time independent.
- The fluid is Newtonian and the solid is isotropic elastic.
- The solid deformation is small such that one-way coupled fluid-structure interaction analysis is valid.

It should be noted that all the above assumptions, except the last one, are also employed in the numerical simulations.

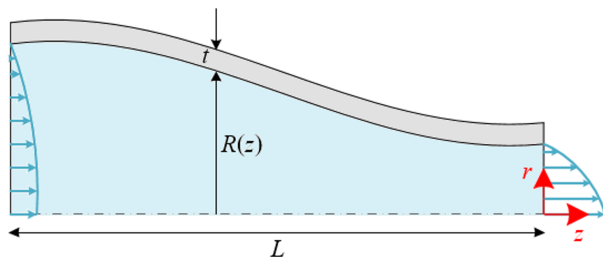


Fig. 1. The problem geometry.

### 2.1. The Fluid Domain

The Navier-Stokes equations, which consist of equations for the mass continuity and the conservation of the momentum, govern the flow of the viscous incompressible fluid. The time-dependent form of these equations reads [28, 29]:

$$\nabla \cdot \mathbf{v} = 0 \quad (1)$$

$$\rho_f \left( \frac{\partial \mathbf{v}}{\partial t} + (\mathbf{v} \cdot \nabla) \mathbf{v} \right) - \mu \nabla^2 \mathbf{v} + \nabla p = \rho_f \mathbf{b}_f \quad (2)$$

Here,  $t$  is time,  $\rho_f$  is the fluid density,  $\mathbf{v}$  and  $p$  represent the fluid velocity and pressure fields,  $\mu$  denotes the fluid viscosity, and  $\mathbf{b}_f$  is the volume force per unit mass of the fluid. When the problem is not time-dependent and volume forces are absent  $\mathbf{b}_f = 0$ , the following steady form of the Navier-Stokes equations can be used [28, 29]:

$$\nabla \cdot \mathbf{v} = 0 \quad (3)$$

$$\nabla p = \mu \nabla^2 \mathbf{v} - \rho_f (\mathbf{v} \cdot \nabla) \mathbf{v} \quad (4)$$

In axisymmetric flows, one can write Eqs. (3) and (4) in terms of radial ( $r$ ) and axial ( $z$ ) coordinates as:

$$\frac{1}{r} \frac{\partial}{\partial r} (r v_r) + \frac{\partial v_z}{\partial z} = 0 \quad (5)$$

$$\begin{aligned} \frac{\partial p}{\partial r} = \mu \left( \frac{1}{r} \frac{\partial}{\partial r} \left( r \frac{\partial v_r}{\partial r} \right) - \frac{v_r}{r^2} + \frac{\partial^2 v_r}{\partial z^2} \right) \\ - \rho_f \left( v_r \frac{\partial v_r}{\partial r} + v_z \frac{\partial v_r}{\partial z} \right) \end{aligned} \quad (6)$$

$$\begin{aligned} \frac{\partial p}{\partial z} = \mu \left( \frac{1}{r} \frac{\partial}{\partial r} \left( r \frac{\partial v_z}{\partial r} \right) + \frac{\partial^2 v_z}{\partial z^2} \right) \\ - \rho_f \left( v_r \frac{\partial v_z}{\partial r} + v_z \frac{\partial v_z}{\partial z} \right) \end{aligned} \quad (7)$$

In order to solve Navier-Stokes equations, appropriate boundary conditions are required. For this purpose, the reference pressure is prescribed to have zero value at the outflow [6, 36]:

$$p = 0 \quad \text{at} \quad z = 0 \quad (8)$$

The following axial velocity ( $v_z$ ) profile is also prescribed at each point of the fluid domain:

$$v_z = v_{\max}(z) \left( 1 - \left( \frac{r}{R(z)} \right)^n \right) \quad (9)$$

In this relation,  $R(z)$  is the radius of the fluid domain at the FSI interface, and  $n = 20$  gives the best fit to the experimental data presented in [37] for internal flow through an axisymmetric constriction. Furthermore, this velocity profile satisfies the no-slip boundary condition (kinematic constraint) at the solid-fluid interface, i.e. [38]:

$$v_z = 0 \quad \text{at} \quad r = R(z) \quad (10)$$

The maximum velocity in each point,  $v_{\max}(z)$ , can be found in terms of the flow rate,  $Q$ , by following relation:

$$Q = \int_0^R 2\pi r v_2 dr = \int_0^R 2\pi r v_{\max}(z) \left(1 - \left(\frac{r}{R(z)}\right)^n\right) dr \quad (11)$$

Evaluating this integral gives:

$$v_{\max}(z) = \frac{n+2}{n} \frac{Q}{\pi R^2} \quad (12)$$

Substituting for  $v_z$  from Eq. (9) back into Eq. (5) and integrating with respect to  $r$  gives  $v_r$ . The integration constant is determined by applying the no-slip boundary condition at FSI interface:

$$v_r = 0 \quad \text{at} \quad r = R(z) \quad (13)$$

After determination of  $v_z$  and  $v_r$ , Eq. (6) can be integrated to obtain the fluid pressure  $p$ . The integration constant is then determined by replacing the relation obtained for  $p$  in Eq. (??) and applying the outflow boundary condition given in Eq. (8).

## 2.2. The Solid Domain

The differential equation of equilibrium for a deformable solid is given by [28, 29]:

$$\nabla \cdot \boldsymbol{\sigma} + \rho_s \mathbf{b}_s = 0 \quad (14)$$

Here,  $\boldsymbol{\sigma}$  is the Cauchy stress tensor,  $\rho_s$  is the solid density and  $\mathbf{b}_s$  is the volume force per unit mass of solid. For axisymmetric problems, in the absence of volume forces, the equilibrium equations reduce to [39]:

$$\frac{\partial \sigma_r}{\partial r} + \frac{\sigma_r - \sigma_\theta}{r} = 0 \quad (15)$$

$$\frac{\partial \tau_{rz}}{\partial r} + \frac{\partial \sigma_z}{\partial z} + \frac{\tau_{rz}}{r} = 0 \quad (16)$$

The constitutive stress-strain relationship for an isotropic elastic solid is expressed as [39]:

$$\boldsymbol{\sigma} = \frac{E}{1+\nu} \boldsymbol{\varepsilon} + \frac{\nu E}{(1+\nu)(1-2\nu)} \varepsilon_{kk} \mathbf{I} \quad (17)$$

where  $E$  is the elasticity modulus,  $\nu$  is the Poisson's ratio,  $\boldsymbol{\varepsilon}$  is the infinitesimal strain tensor,  $\varepsilon_{kk}$  is the first scalar invariant of  $\boldsymbol{\varepsilon}$  and  $\mathbf{I}$  denotes the unit tensor. For axisymmetric analysis, this equation gives:

$$\sigma_r = \frac{E}{(1+\nu)} \left[ \varepsilon_r + \frac{\nu}{1-2\nu} (\varepsilon_r + \varepsilon_\theta + \varepsilon_z) \right] \quad (18)$$

$$\sigma_\theta = \frac{E}{(1+\nu)} \left[ \varepsilon_\theta + \frac{\nu}{1-2\nu} (\varepsilon_r + \varepsilon_\theta + \varepsilon_z) \right] \quad (19)$$

$$\sigma_z = \frac{E}{(1+\nu)} \left[ \varepsilon_z + \frac{\nu}{1-2\nu} (\varepsilon_r + \varepsilon_\theta + \varepsilon_z) \right] \quad (20)$$

$$\tau_{rz} = \frac{E}{(1+\nu)} \varepsilon_{rz} \quad (21)$$

Strain components are also given by [39]:

$$\begin{aligned} \varepsilon_r &= \frac{\partial u}{\partial r}, & \varepsilon_\theta &= \frac{u}{r}, \\ \varepsilon_z &= \frac{\partial w}{\partial z}, & \varepsilon_{rz} &= \frac{1}{2} \left( \frac{\partial u}{\partial z} + \frac{\partial w}{\partial r} \right) \end{aligned} \quad (22)$$

where  $u$  and  $w$  are displacement components in the radial and axial directions. Substituting from Eq. (22) back into Eqs. (18-21) yields:

$$\sigma_r = \frac{E}{(1+\nu)} \left[ \frac{\partial u}{\partial r} + \frac{\nu}{1-2\nu} \left( \frac{\partial u}{\partial r} + \frac{u}{r} + \frac{\partial w}{\partial z} \right) \right] \quad (23)$$

$$\sigma_\theta = \frac{E}{(1+\nu)} \left[ \frac{u}{r} + \frac{\nu}{1-2\nu} \left( \frac{\partial u}{\partial r} + \frac{u}{r} + \frac{\partial w}{\partial z} \right) \right] \quad (24)$$

$$\sigma_z = \frac{E}{(1+\nu)} \left[ \frac{\partial w}{\partial z} + \frac{\nu}{1-2\nu} \left( \frac{\partial u}{\partial r} + \frac{u}{r} + \frac{\partial w}{\partial z} \right) \right] \quad (25)$$

$$\tau_{rz} = \frac{E}{2(1+\nu)} \left( \frac{\partial u}{\partial z} + \frac{\partial w}{\partial r} \right) \quad (26)$$

Replacing from these relations into equilibrium equations, Eqs. (15) and (16), gives the system of partial differential equations governing the deformation of the solid domain:

$$\begin{aligned} (1-\nu) \left( \frac{\partial^2 u}{\partial r^2} + \frac{1}{r} \frac{\partial u}{\partial r} - \frac{u}{r^2} \right) + \nu \frac{\partial^2 w}{\partial z \partial r} &= 0 \\ \frac{\partial^2 u}{\partial r \partial z} + \frac{1}{r} \frac{\partial u}{\partial z} + (1-2\nu) \left( \frac{\partial^2 w}{\partial r^2} + \frac{1}{r} \frac{\partial w}{\partial r} \right) &+ (2-2\nu) \frac{\partial^2 w}{\partial z^2} = 0 \end{aligned} \quad (27)$$

The following set of boundary conditions is employed for solving these equations:

$$\sigma_r = p \quad \text{at} \quad r = R(z) \quad (28)$$

$$\sigma_r = 0 \quad \text{at} \quad r = R(z) + t \quad (29)$$

$$\tau_{rz} = -\mu \frac{\partial v(r, z)}{\partial z} \quad \text{at} \quad r = R(z) \quad (30)$$

$$\tau_{rz} = 0 \quad \text{at} \quad r = R(z) + t \quad (31)$$

$$\sigma_z = 0 \quad \text{for a tube with free ends} \quad (32)$$

$$\varepsilon_z = 0 \quad \text{for a tube with free ends} \quad (33)$$

In these relations,  $t$  is the solid thickness. The effect of the fluid pressure normal load and viscous tangential load on the solid structure (dynamic constraint) is accounted for by imposing the boundary conditions given in Eqs. (30) and (32), respectively. Finally, the set of equations presented above for the fluid and structure domains was solved by means of Matlab symbolic toolbox.

One of the most important advantages of the above methodology is that once the associated Matlab code is developed, it can be used to solve different FSI

problems in axisymmetric domain just by adjusting the FSI interface function  $R(z)$  and domain boundary conditions. While in numerical simulations, solving a new problem requires to define the geometrical model and mesh its domain which is time-consuming and labor-intensive. However, as mentioned earlier, the above-developed analytical approach is a one-way coupled fluid-structure interaction analysis, since it only accounts for the loads applied to the solid structure from the fluid part in the FSI interface. The effect of structure deformation on moving the fluid interface is not captured in this methodology. Consequently, this methodology is best-suited for analysis of FSI systems in which deformation of the solid structure is small. Many real-world problems like stress analysis in fluid transporting tubes are among such FSI systems.

**2.3. Results and Discussions**

**2.4. Cylindrical Pressure Vessel**

In thick cylindrical pressure vessels, it is assumed that  $u \equiv u(r)$ . Moreover, the fluid pressure is constant, i.e.  $p = cte$ , and it can be assumed that  $\mu = 0$  since the fluid is stationary. Substituting these relations back into Eqs. (27-30) gives:

$$\begin{aligned} \frac{d^2u}{dr^2} + \frac{1}{r} \frac{du}{dr} - \frac{u}{r^2} &= 0 \\ \sigma_r &= p \quad \text{at} \quad r = R(z) \\ \sigma_r &= 0 \quad \text{at} \quad r = R(z) + t \end{aligned} \tag{34}$$

Solving this differential equation and applying the boundary conditions gives:

$$u = \frac{1 - \nu}{E(R_o^2 - R_i^2)} \left( \frac{R_i^2 p}{r} - \frac{R_i^2 R_o^2 p}{2r} \right) \tag{35}$$

This relation that can be found in many related texts such as [40] proves the capability of the derived methodology in this simple example.

**2.5. Flow Through a Nozzle**

The relationship between the wall deformation and the fluid dynamics in nozzles is important for medical and engineering applications [41]. Here, the relations developed in section 2 are employed to obtain the fluid and solid responses in flow through a nozzle with a curved profile. The nozzle geometry is given in Fig. 2. The fluid material is water with  $\rho_f = 1000 \text{ kg/m}^3$  and  $\mu = 8.90 \times 10^{-4} \text{ Pa.s}$ , while the solid is made of Aluminum with  $E = 70 \text{ GPa}$  and  $\nu = 0.33$ .

In this figure, the nozzle inlet and outlet radii are  $R_1 = 0.15\text{m}$ ,  $R_2 = 0.05\text{m}$  and its length and wall thickness are  $L = 0.386\text{m}$  and  $t = 0.01\text{m}$ , respectively. The nozzle radius  $R(z)$  is given by:  $R(z) = 0.7038z^2 + 0.0126z + 0.05$ . Fig. 3 defines lines 1 to 5,

which are used later in this section for presentation of results.

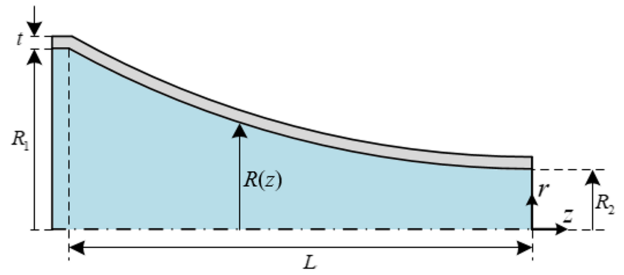


**Fig. 2.** The nozzle geometry.

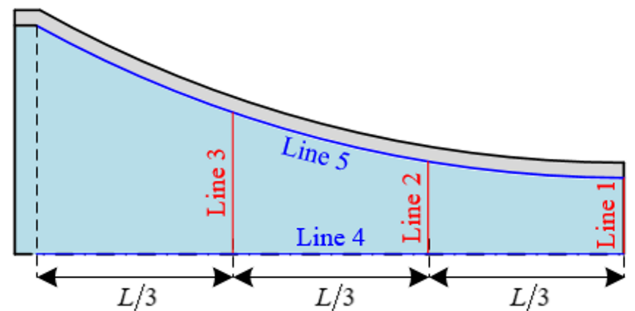


**Fig. 3.** Definition of lines 1 to 5 for presentation of results.

The results are compared to results of numerical simulations performed by ANSYS/CFX software. For numerical analysis, the mesh sensitivity test is performed for hoop stress in the nozzle wall at  $z = -0.3\text{m}$  along line 5. The results of this test are presented in Fig. 4. After performing the mesh sensitivity, 14400 FLUID141 (2D 4-Node quadrilateral fluid) elements and 1260 PLANE182 (2D 4-Node quadrilateral structural solid) elements were selected to mesh fluid and solid domains, respectively.

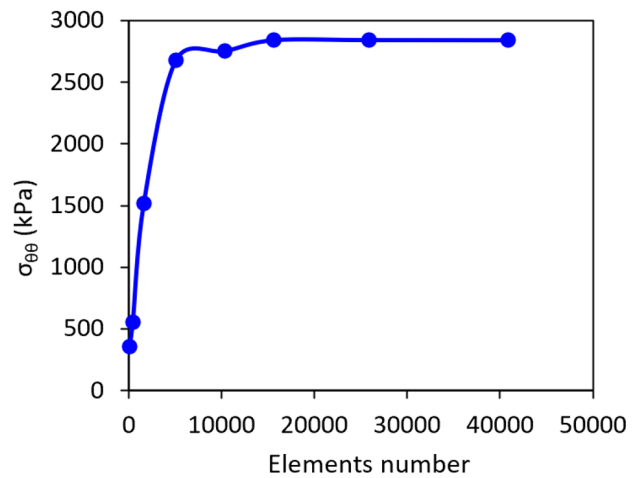


**Fig. 4.** Results of the mesh sensitivity analysis.

A coarse version of the finite element mesh is presented in Fig. 5. The boundary conditions on different boundaries of Fig. 5 are as follows: on boundary 1 an inlet velocity is prescribed, on boundary 2 the outlet

pressure is specified, on boundary 3 the axisymmetric conditions are applied, on boundary 4 the FSI interface conditions are enforced, and finally on boundaries 5 and 6 the displacement of the solid domain is fixed. The initial conditions of  $v = 0\text{m/s}$  and  $p = 0\text{Pa}$  are prescribed everywhere in the fluid domain.

Analytical and numerical solutions for flow axial and radial velocities along different lines of Fig. 3 are compared in Figs. 6 and 7. Note that the radial velocity is zero along line 1.

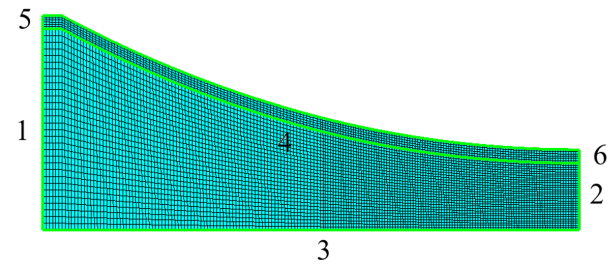


Fig. 5. A coarse version of the finite element mesh.

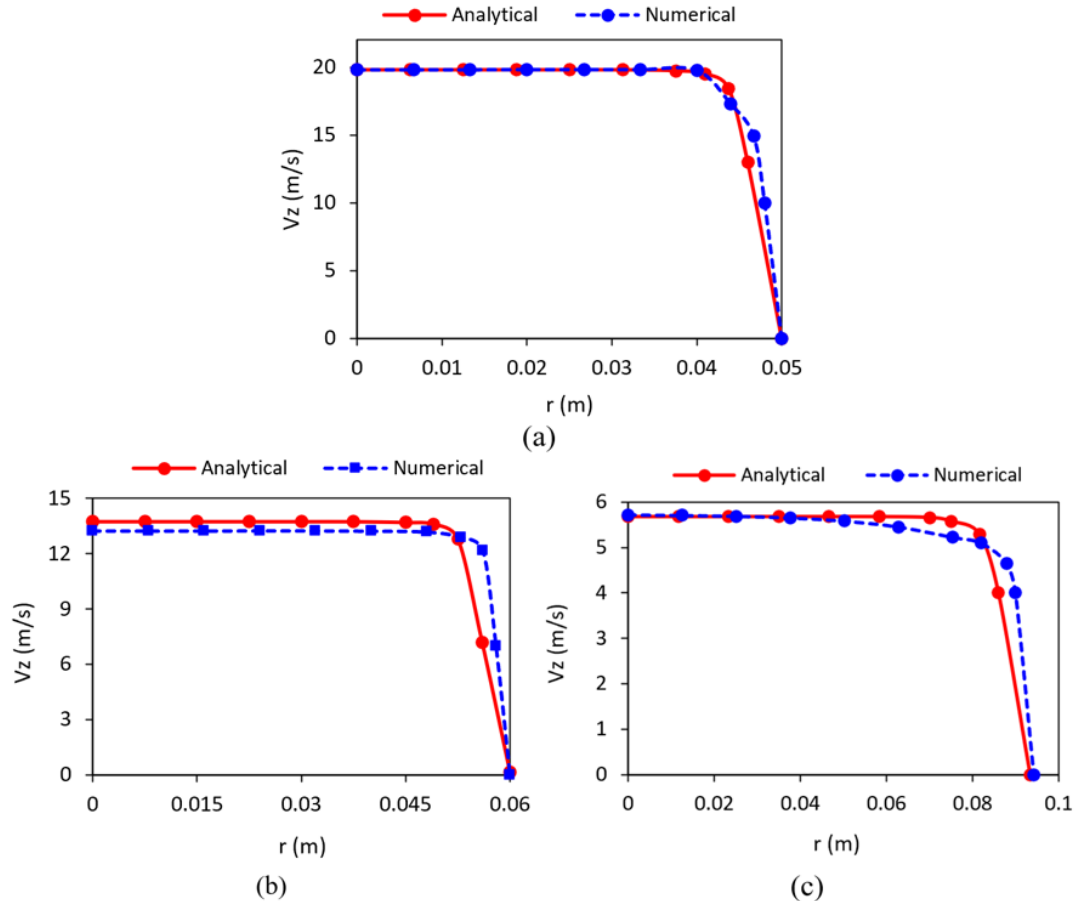


Fig. 6. The flow axial velocity variation along a) line 1, b) line 2, and c) line 3.

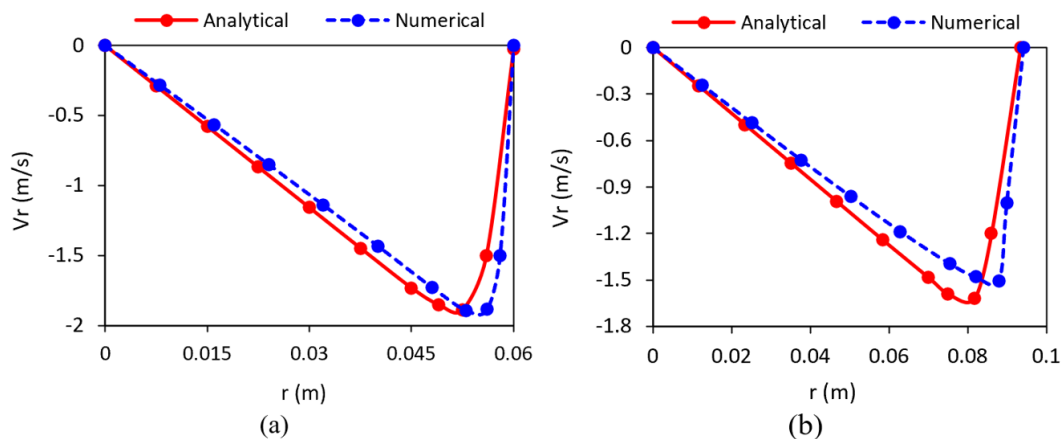


Fig. 7. The flow radial velocity variation along a) line 2, b) line 3.

The fluid pressure distribution in axial direction is also compared for analytical and numerical approaches in Fig. 8.

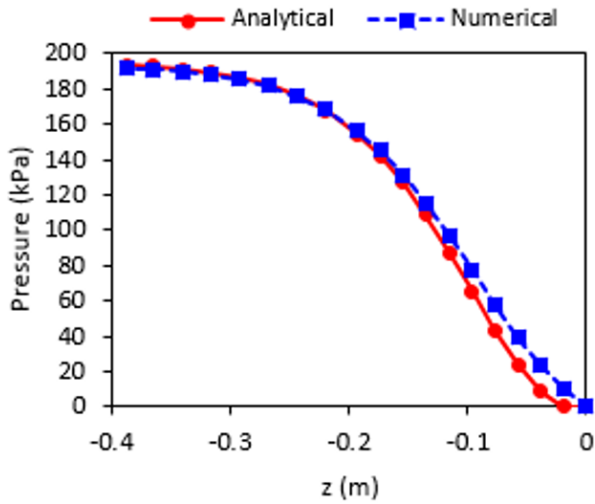


Fig. 8. The flow pressure variation along line 4.

According to Figs. 6 to 8, analytical and numerical data are in good agreement, especially near the nozzle centerline, i.e.  $r = 0$ . The difference between analytical and numerical results near the nozzle wall, i.e.  $r = R(z)$ , is mainly due to the axial velocity profile assumed in Eq. (9) for the analytical approach. While this velocity profile can accurately predict the maximum flow velocity that occurs near the centerline, it gives a thicker boundary layer near the nozzle wall. Consequently, the analytically calculated velocity is higher in these regions to give equal flow rate with the numerical method. On the other hand, the analytical pressure is lower in these regions due to the Bernoulli principle.

Contours of the flow velocity and pressure distribution in the nozzle obtained by the numerical simulation are given in Fig. 9.

The results of analytical and numerical approaches for different stress components along line 5 are compared in Fig. 10. The contour of the hoop stress distribution in the nozzle wall is also given in Fig. 11.

Here, it is worth mentioning that all analyses were performed on an ASUS laptop model N552V with Intel-Core i7-6700HQ CPU and 12GB of RAM. The construction of the numerical model for the nozzle problem in ANSYS took about 4 hours to be completed by author, while its solution time by ANSYS was about 8 minutes. However, the modification of the Matlab code for analytical modeling of the nozzle problem took less than 10 minutes to be performed by author, while its solution time by Matlab was less than 1 minute. This comparison clearly shows that it takes much less time and labor to prepare the analytical model and furthermore, its runtime is smaller than that of the numerical model. Moreover, comparisons made in Figs. 6, 7, 8, and 10 between the results of analytical and numerical models demonstrate the capability of the analytical model to solve the FSI problems with minimal error. However, despite its advantages, the proposed analytical method has some limits. The most important limits are:

- The method can be used to solve FSI problems only when the problem domain is axisymmetric,
- It is not applicable to time-dependent problems,
- It applies a one-way coupled fluid-structure interaction scheme, so its accuracy is reasonable only if the solid deformation is small.

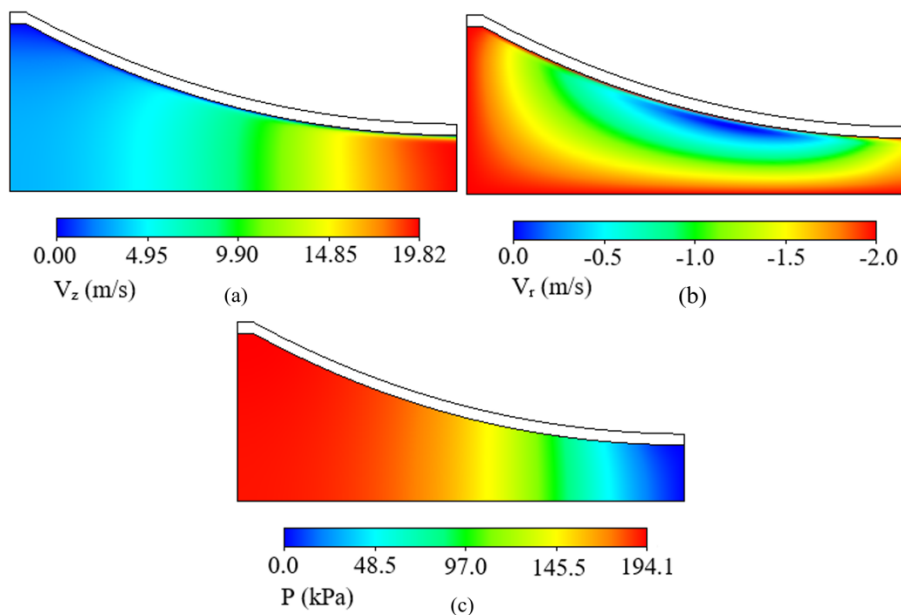
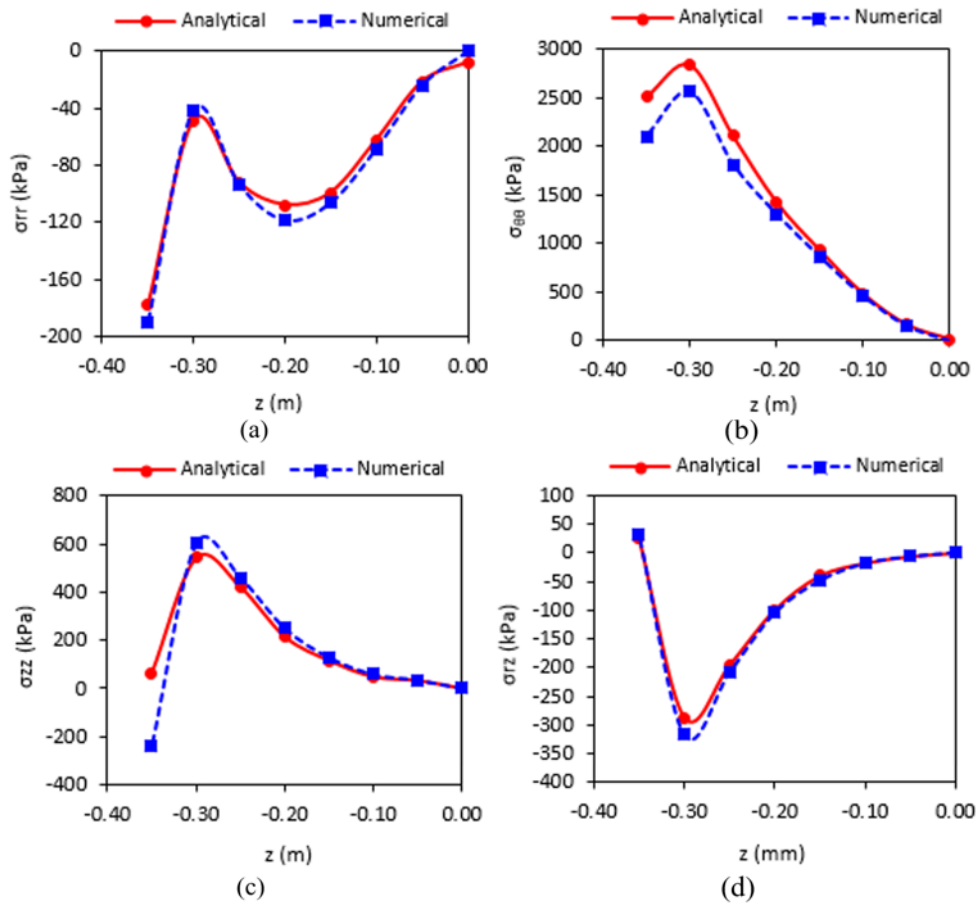
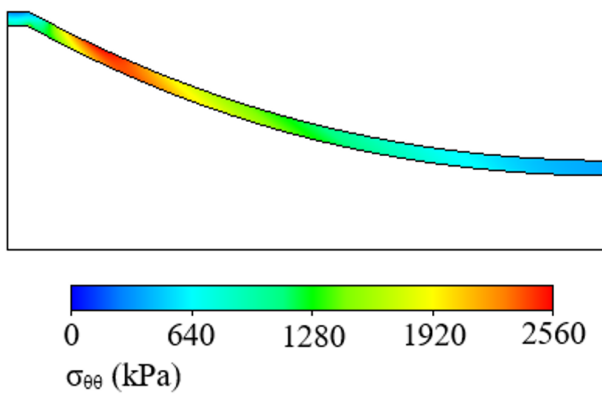


Fig. 9. Contours of the flow a) axial velocity, b) radial velocity, and c) pressure distribution.



**Fig. 10.** The variation of a) radial stress, b) hoop stress, c) axial stress, and d) shear stress along line 5 on the nozzle wall.



**Fig. 11.** Contour of the hoop stress distribution in the nozzle wall.

### 3. Conclusions

In this paper, an analytical approach was proposed to model Fluid-structure interaction problems in axisymmetric domains. In this approach, the flow of the incompressible viscous fluid is described by steady Navier-Stokes equations, while the stationary momentum equations govern the solid structure, which is as-

sumed to have linear elastic behavior. The kinematic constraint, i.e. the no-slip condition for fluid flow, and the dynamic constraint, i.e. the fluid pressure normal force and viscous tangential force on the structure, are imposed on the fluid-structure interface by introducing appropriate boundary conditions. The validity of this approach was proved in two different ways. In the first way, the analytical equations were specialized for the simple case of thick cylindrical vessels. In the second way, the presented approach was further verified by comparing its results for flow through a nozzle with results of the numerical simulation of the problem. The developed approach can be used for fast solution of fluid-structure interaction problems in axisymmetric configuration with reasonable accuracy.

### Conflict of Interest

None declared.

### Acknowledgements

The Author acknowledges the funding support of Babol Noshirvani University of Technology through Grant

Program No. BNUT/389003/97.

## References

- [1] D. Cinquegrana, P.L. Vitagliano, Validation of a new fluid-structure interaction framework for non-linear instabilities of 3D aerodynamic configurations, *J. Fluids Struct.*, 103 (2021) 103264.
- [2] E. Alaei, H. Afrasiab, M. Dardel, Analytical and numerical fluid-structure interaction study of a microscale piezoelectric wind energy harvester, *Wind Energy.*, 23(6) (2020) 1444-1460.
- [3] S. Meduri, M. Cremonesi, A. Frangi, U. Perego, A lagrangian fluid-structure interaction approach for the simulation of airbag deployment, *Finite Elem. Anal. Des.*, 198 (2022) 103659.
- [4] J. Boustani, M.F. Barad, C.C. Kiris, C. Brehm, An immersed boundary fluid-structure interaction method for thin, highly compliant shell structures, *J. Comput. Phys.*, 438 (2021) 110369.
- [5] A. Morvan, M. Sacher, A. Nème, J.B. Leroux, C. Jochum, N. Abiven, Efficient jib-mainsail fluid-structure interaction modelling Validations with semi-rigid sails experiments, *Ocean Eng.*, 243 (2022) 110210.
- [6] H. Afrasiab, M.R. Movahhedy, A. Assempour, Proposal of a new design for valveless micropumps, *Sci. Iran.*, 18(6) (2011) 1261-1266.
- [7] H. Safi, N. Phillips, Y. Ventikos, R. Bomphrey, Implementing fluid-structure interaction computational and empirical techniques to assess hemodynamics of abdominal aortic aneurysms, *Artery Res.*, 20(C) (2017) 55-56.
- [8] M. Kazemiyani, H. Afrasiab, M.H. Pashaei, Comparison of the plaque rupture risk in different double-stenosis arrangements of coronary arteries by modeling fluid-structure interaction, *Modares Mech. Eng.*, 16(2) (2016) 10-18.
- [9] Z. Xie, X. Wang, W. Zhu, Theoretical and experimental exploration into the fluid structure coupling dynamic behaviors towards water-lubricated bearing with axial asymmetric grooves, *Mech. Syst. Signal Process.*, 168 (2022) 108624.
- [10] J. Pirnar, B. Širok, A. Bombač, Effect of airway surface liquid on the forces on the pharyngeal wall: Experimental fluid-structure interaction study, *J. Biomech.*, 63 (2017) 117-124.
- [11] T. Gleim, P. Birken, M. Weiland, D. Kuhl, A. Meister, O. Wünsch, Experimental and numerical aspects of a thermal fluid-structure phenomenon, *AIP Conf. Proc.*, 1863(1) (2017) 410004.
- [12] A. Hessenthaler, N.R. Gaddum, O. Holub, R. Sinkus, O. Röhrle, D. Nordsetten, Experiment for validation of fluid-structure interaction models and algorithms, *Int. J. Numer. Methods Biomed. Eng.*, 33(9) (2017) e2848.
- [13] P.B. Ryzhakov, E. Oñate, A finite element model for fluid-structure interaction problems involving closed membranes, internal and external fluids, *Comput. Methods Appl. Mech. Eng.*, 326 (2017) 422-445.
- [14] M. Abbadeni, I. Zidane, H. Zahloul, A. Fatu, M. Hajjam, Finite element analysis of fluid-structure interaction in the hydromechanical deep drawing process, *J. Mech. Sci. Technol.*, 31(11) (2017) 5485-5491.
- [15] A.K. Slone, K. Pericleous, C. Bailey, M. Cross, Dynamic fluid-structure interaction using finite volume unstructured mesh procedures, *Comput. Struct.*, 80(5-6) (2002) 371-390.
- [16] D.R. Wilkes, A.J. Duncan, Acoustic coupled fluid-structure interactions using a unified fast multipole boundary element method, *J. Acoust. Soc. Am.*, 137(4) (2015) 2158-2167.
- [17] H. Yao, H. Zhang, H. Liu, W. Jiang, Numerical study of ow-excited noise of a submarine with full appendages considering fluid structure interaction using the boundary element method, *Eng. Anal. Bound. Elem.*, 77 (2017) 1-9.
- [18] L. Wang, G.M.D. Currao, F. Han, A.J. Neely, J. Young, F.-B. Tian, An immersed boundary method for fluid-structure interaction with compressible multiphase ows, *J. Comput. Phys.*, 346 (2017) 131-151.
- [19] A. Gerstenberger, W.A. Wall, An extended finite element method/lagrange multiplier based approach for fluid-structure interaction, *Comput. Methods Appl. Mech. Eng.*, 197(19-20) (2008) 1699-1714.
- [20] D.J. Munk, T. Kipouros, G.A. Vio, G.P. Steven, G.T. Parks, Topology optimisation of micro fluidic mixers considering fluid-structure interactions with a coupled lattice Boltzmann algorithm, *J. Comput. Phys.*, 349 (2017) 11-32.
- [21] A. Zhang, P. Sun, F. Ming, A. Colagrossi, Smoothed particle hydrodynamics and its applications in fluid-structure interactions, *J. Hydrodyn. Ser B.*, 29(2) (2017) 187-216.
- [22] D. Soares Jr., Fluid-structure interaction analysis by optimised boundary element-finite element coupling procedures, *J. Sound Vib.*, 322(1-2) (2009) 184-195.

- [23] X. Cui, X. Yao, Z. Wang, M. Liu, A hybrid wavelet-based adaptive immersed boundary finite-difference lattice Boltzmann method for two-dimensional fluid-structure interaction, *J. Comput. Phys.*, 333 (2017) 24-48.
- [24] Z. Li, J. Favier, A non-staggered coupling of finite element and lattice Boltzmann methods via an immersed boundary scheme for fluid-structure interaction, *Comput. Fluids.*, 143 (2017) 90-102.
- [25] Z. Li, J. Leduc, A. Combescure, F. Leboeuf, Coupling of SPH-ALE method and finite element method for transient fluid-structure interaction, *Comput. Fluids.*, 103 (2014) 6-17.
- [26] D. Hu, T. Long, Y. Xiao, X. Han, Y. Gu, Fluid-structure interaction analysis by coupled FE-SPH model based on a novel searching algorithm, *Comput. Methods Appl. Mech. Eng.*, 276 (2014) 266-286.
- [27] J.R. Craig, W. Wayne Read, The future of analytical solution methods for groundwater flow and transport simulation, XVIII International Conference on Water Resources (CMWR), Barcelona, (2010).
- [28] H. Afrasiab, M.R. Movahhedy, Treatment of the small time instability in the finite element analysis of fluid structure interaction problems, *Int. J. Numer. Methods Fluids.*, 71(6) (2013) 756-771.
- [29] H. Afrasiab, M.R. Movahhedy, A. Assempour, Fluid-structure interaction analysis in micro microfluidic devices: A dimensionless finite element approach, *Int. J. Numer. Methods Fluids.*, 68(9) (2012) 1073- 1086.
- [30] P. Xu, P.R. Wellens, Theoretical analysis of nonlinear fluid-structure interaction between large-scale polymer offshore coating photovoltaics and waves, *Ocean Eng.*, 249 (2022) 110829.
- [31] S. Soni, N.K. Jain, P.V. Joshi, A. Gupta, Effect of fluid-structure interaction on vibration and deflection analysis of generally orthotropic submerged micro-plate with crack under thermal environment: an analytical approach, *J. Vib. Eng. Technol.*, 8 (2020) 643-672.
- [32] M. Fritsche, P. Epple, A. Delgado, Analytical and numerical investigation of the fluid structure interaction of an elastic beam in a water channel, Proceedings of the ASME (American Society of Mechanical Engineers Digital Collection) 2020 International Mechanical Engineering Congress and Exposition. Volume 10: Fluids Engineering. Virtual, Online. November 16-19, (2020) V010T10A049.
- [33] N.K. Jain, S. Soni, R. Prajapati, Analytical treatment for vibration analysis of partially cracked orthotropic and FGM submerged cylindrical shell with consideration of fluid-structure interaction, *Mech. Based Des. Struct. Mach.*, 49(4) (2021) 463-486.
- [34] C.-C. Yu, A.S. Whittaker, Review of analytical studies on seismic fluid-structure interaction of base-supported cylindrical tanks, *Eng. Struct.*, 233 (2021) 111589.
- [35] C. Zhang, Fluid-structure interaction in rectilinear flows: Four analytical solutions, *Phys. Fluids.*, 33(6) (2021) 063611.
- [36] H. Afrasiab, M.R. Movahhedy, A. Assempour, Finite element and analytical fluid-structure interaction analysis of the pneumatically actuated diaphragm microvalves, *Acta Mech.*, 222 (2011) 175.
- [37] A. Van Hirtum, B. Wu, H. Gao, X.Y. Luo, Constricted channel flow with different cross-section shapes, *Eur. J. Mech. - B/Fluids.*, 63 (2017) 1-8.
- [38] A. Sohankar, A. Joulaei, M. Mahmoodi, Fluid flow and convective heat transfer in a rotating rectangular microchannel with various aspect ratios, *Int. J. Therm. Sci.*, 172 (Part A) (2022) 107259.
- [39] A.P. Boresi, K.P. Chong, J.D. Lee, *Elasticity in Engineering Mechanics*, John Wiley and Sons, (2010).
- [40] V. Vullo, *Circular Cylinders and Pressure Vessels: Stress Analysis and Design*, 2nd ed., Springer Science and Business Media, (2016).
- [41] S. Murugappan, E.J. Gutmark, R.R. Lakshmanraj, S. Khosla, Flow-structure interaction effects on a jet emanating from a flexible nozzle, *Phys. Fluids.*, 20(11) (2008) 117105.